© 2022. Published by The Company of Biologists Ltd | Journal of Cell Science (2022) 135, jcs260627. doi:10.1242/jcs.260627

RESEARCH ARTICLE

SHARPIN S146 phosphorylation mediates ARP2/3 interaction, cancer cell invasion and metastasis

Umar Butt[1,2], Meraj H. Khan[2], Jeroen Pouwels[2] and Jukka Westermarck[1,2,*]

ABSTRACT

SHARPIN is involved in several cellular processes and promotes cancer progression. However, how the choice between different functions of SHARPIN is post-translationally regulated is unclear. Here, we characterized SHARPIN phosphorylation by mass spectrometry and *in vitro* kinase assay. Focusing on S131 and S146, we demonstrate that they have a role in SHARPIN-ARP2/3 complex interaction, but play no role in integrin inhibition or LUBAC activation. Consistent with its novel role in ARP2/3 regulation, S146 phosphorylation of SHARPIN promoted lamellipodia formation. We also demonstrate that SHARPIN S146 phosphorylation-mediated ARP2/3 interaction is sensitive to inhibition of ERK1/2 or reactivation of protein phosphatase 2A (PP2A). Notably, CRISPR/Cas9-mediated knockout of SHARPIN abrogated three-dimensional (3D) invasion of several cancer cell lines. The 3D invasion of cancer cells was rescued by overexpression of the wild-type SHARPIN, but not by SHARPIN S146A mutant. Finally, we demonstrate that inhibition of phosphorylation at S146 significantly reduces *in vivo* metastasis in a zebrafish model. Collectively, these results map SHARPIN phosphorylation sites and identify S146 as a novel phosphorylation switch defining ARP2/3 interaction and cancer cell invasion.

This article has an associated First Person interview with the first author of the paper.

KEY WORDS: FRET, Invasion, LUBAC, MDA-MB-231, Integrin, Phosphorylation

INTRODUCTION

The primary cause for cancer-related deaths is metastasis (Steeg, 2016). Significant improvements in cancer survival rates have been seen recently due to early diagnosis and development of targeted therapies (Guan, 2015). Metastasis, however, remains a hurdle that most cancer therapies are not able to overcome. Cancer metastasis involves several critical steps. First, the cancer cell(s) needs to detach from the primary tumor. Subsequentially, the detached cell needs to migrate into and through the surrounding tissue, a step called invasion. Then, the metastasizing cancer cell needs to travel through the blood or lymph system, after which it needs to adhere to the secondary site, where it once more needs to invade to reach its final destination (Fares et al., 2020). Suppressing cancer metastasis by targeting any of these processes would be of urgent therapeutic need (Ganesh and Massagué, 2021). However, this would require a detailed mechanistic understanding of how these processes are regulated and, consequently, identification of potential target mechanisms for anti-metastatic therapies.

SHANK-associated RH domain interactor (SHARPIN) is mainly a cytoplasmic adaptor protein involved in the regulation of multiple cellular functions (De Franceschi et al., 2015; Gao et al., 2019; Jung et al., 2010; Khan et al., 2017; Liu et al., 2017; Park et al., 2016; Rantala et al., 2011; Zhang et al., 2014; Zhou et al., 2020). The most explored function of SHARPIN is its interaction with RBCK1 (HOIL) and RNF31 (HOIP) to form the linear ubiquitin chain assembly complex (LUBAC), a regulator of the canonical NF-κB pathway signaling (Gerlach et al., 2011; Ikeda et al., 2011; Tokunaga et al., 2011). SHARPIN is also well known as an important inactivator of integrins (Pouwels et al., 2013; Rantala et al., 2011). Other molecular targets of SHARPIN include T-cell receptor, caspase 1, EYA transcription factors, SHANK proteins and PTEN (He et al., 2010; Landgraf et al., 2010; Lim et al., 2001; Nastase et al., 2016; Park et al., 2016). Multiple cellular functions indicate that different signaling pathways compete for SHARPIN, and that SHARPIN functions as a signaling coordinator (De Franceschi et al., 2015). However, how differential binding of SHARPIN to its partners is spatio-temporally regulated remains unknown. Post-translational modifications (PTMs) of SHARPIN are likely to be involved, as PTMs are known to function as molecular switches by affecting protein-protein interactions (Chen et al., 2020; Nishi et al., 2011). However, besides the recent identification of S165 phosphorylation of SHARPIN as the activating phosphorylation for LUBAC activation (Thys et al., 2021), the phosphorylation switches determining SHARPIN activity towards different cellular functions remain obscure.

SHARPIN gene is amplified, and SHARPIN protein is overexpressed, in a variety of human cancers (Fig. S1A) (Bii et al., 2015; De Melo and Tang, 2015; He et al., 2010; Jung et al., 2010). The overexpressed SHARPIN promotes cancer cell proliferation, tumor formation and cancer metastasis (Bii et al., 2015; He et al., 2010; Li et al., 2015; Zhang et al., 2014). However, the molecular determinants by which these different cancer-related functions of SHARPIN are regulated are poorly understood. What is known is that SHARPIN regulates cell adhesion and migration by inhibition of integrins (De Franceschi et al., 2015; Pouwels et al., 2013; Rantala et al., 2011), by AKT activation via PTEN inhibition (De Melo et al., 2014; He et al., 2010) or by promotion of lamellipodium formation through the ARP2/3 complex (Khan et al., 2017). The seven-subunit ARP2/3 complex is responsible for creating branched actin networks through polymerization of actin (Blanchoin et al., 2000; Rana et al., 2021). Overexpression of the ARP2/3 complex has been observed in a variety of human cancers (Iwaya et al., 2007; Liu et al., 2013; Otsubo et al., 2004; Semba et al., 2006; Zhang et al., 2012). This overexpression of the ARP2/3 complex is strongly associated with tumor cell invasion

[1]Institute of Biomedicine, University of Turku, Turku, FI-20014, Finland. [2]Turku Bioscience Centre, University of Turku, and Åbo Akademi University, FI-20520, Turku, Finland.

*Author for correspondence (jukwes@utu.fi)

J.W., 0000-0001-7478-3018

Handling Editor: Michael Way
Received 11 September 2022; Accepted 13 September 2022

Journal of Cell Science (2022) 135, jcs260627. doi:10.1242/jcs.260627

(Mondal et al., 2021), and can be used as a marker to differentiate benign lesions and malignant melanomas (Kashani-Sabet et al., 2009). Therefore, understanding the mechanism that activates tumor invasion-promoting ARP2/3 functions could lead to novel therapeutic opportunities for preventing metastasis, which is the dominant cause for death of cancer patients.

Here, we demonstrate that phosphorylation on SHARPIN at S146 promotes cancer cell invasion. This phosphorylation switch selectively mediates SHARPIN interaction with ARP2/3 complex, indicating that this protein interaction might provide a target for therapeutic interference in cancer.

RESULTS

Identification of *in vitro and in cellulo* SHARPIN phosphorylation sites

To better understand SHARPIN phosphorylation in cancer cells, an *in vitro* kinase assay (IVK) was performed with GST-SHARPIN in the presence of active forms of oncogenic kinases PKCα (also known as PRKCA), CDK4/CycD3, FAK (also known as PTK2), ERK1 (also known as MAPK3), ERK2 (also known as MAPK1), AKT1 and AKT2. The autoradiograph revealed that GST-SHARPIN is potentially phosphorylated by PKCα, CDK4/CycD3, ERK1 and ERK2 (Fig. 1A). Mass spectrometry (MS) analysis of these samples confirmed at least one phosphorylation site to be phosphorylated by PKCα, CDK4/CycD3, ERK1 and ERK2, and collectively revealed 12 phospho-sites in GST-SHARPIN regulated by these kinases (Fig. 1B) (Table 1).

To identify which sites on SHARPIN are constitutively phosphorylated in proliferating cells, GFP pulldowns from HEK-293 cells expressing GFP-SHARPIN or GFP alone were analyzed by affinity purification coupled with MS (AP-MS) (Fig. 1B). The MS analysis revealed seven SHARPIN phospho-sites, out of which S131, S146, S165, T309 and S312 were overlapping with IVK sites (Table 1). Several phospho-sites identified here had also been observed by an MS analysis available in the Proteomics Identification Database [‘Identification of novel SHARPIN binders’ (PXD004734)] (Fig. 1B) (Table 1). Moreover, seven phospho-sites of SHARPIN have been reported at https://www.phosphosite.org/proteinAction.action?id=2615758 (Table 1). Table 1 presents current knowledge on SHARPIN phosphorylation, revealing 14 phosphorylation sites from cultured cells and five novel phosphorylation sites identified here by IVK.

SHARPIN amino acid S146 is involved in ARP2/3 complex interaction

We selected ERK1/2 target sites S131 and S146 for further functional analysis based on the following criteria: (1) phosphorylated by oncogenic ERK1/2; (2) presence in both the IVK and *in cellulo* MS analysis (Table 1); and (3) clustering to an unstructured linker region of SHARPIN, the function of which is yet unknown (Fig. 1C). To investigate the functional role of S131 and S146 phosphorylation, we created alanine mutants of these phospho-sites in a GFP-SHARPIN mammalian expression vector. Upon transient transfection, both mutants were overexpressed at comparable levels as wild-type (WT) GFP-SHARPIN when assessed by western blotting (WB) (Fig. S1B,C). As functional read-outs, we used previously established assays for three SHARPIN-regulated functions: integrin activity, LUBAC activity and ARP2/3 interaction (Bouaouina et al., 2011; Harburger et al., 2009; Khan et al., 2017).

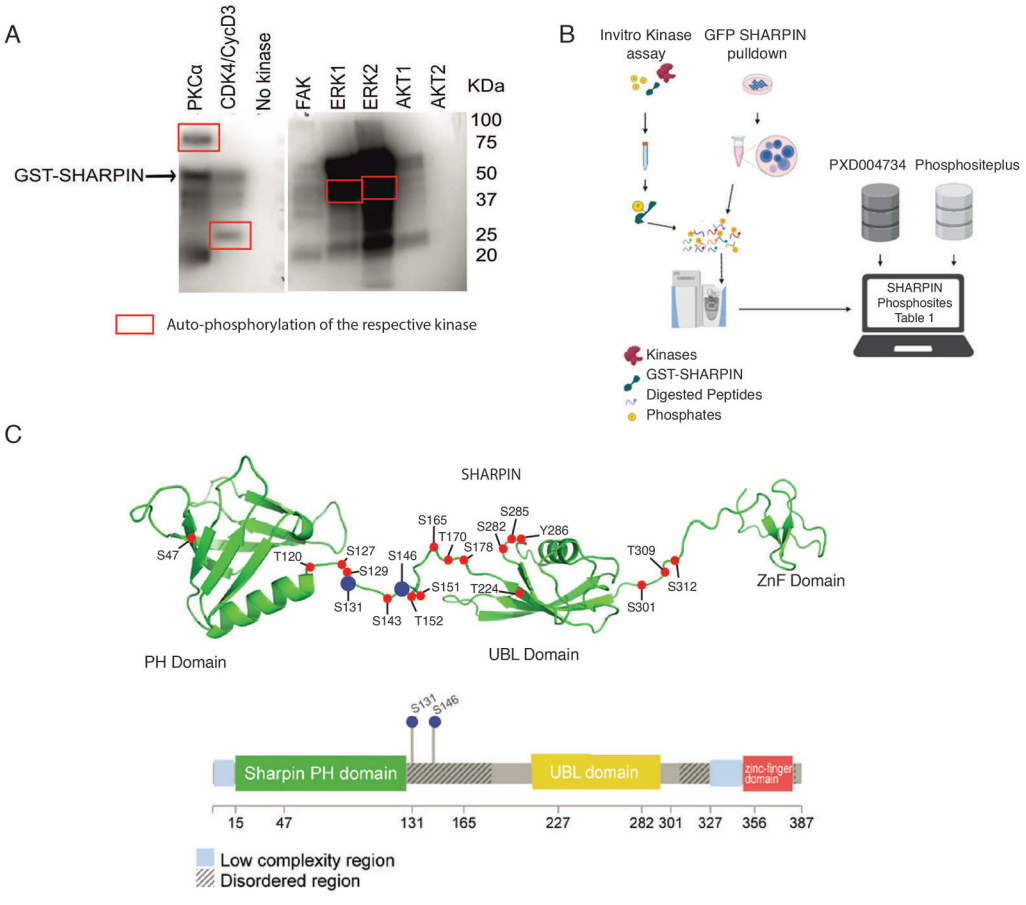

Fig. 1. Phosphorylation of SHARPIN. (A) SHARPIN phosphorylation by oncogenic kinases (PKCα, CDK4/CycD3, ERK1 and ERK2) in an *in vitro* kinase assay (IVK). (B) Schematic of approaches used for comprehensive analysis of SHARPIN phosphorylation. (C) SHARPIN phosphorylation sites (blue) on a cartoon model illustrating the individual functional domains connected by a linker region (top), and a lollipop diagram of SHARPIN showing phosphorylation sites in the disordered region selected for further analysis (bottom).

Journal of Cell Science (2022) 135, jcs260627. doi:10.1242/jcs.260627

Table 1. Summary of SHARPIN phosphorylation sites

Phospho-site	IVK or *in cellulo*	Kinases in IVK	PRIDE PXD004734	PhosphoSitePlus®
S47	IVK	ERK1+2		
T120			YES	
S127			YES	
S129	*in cellulo*		YES	
S131	IVK/*in cellulo*	ERK1+2, CDK4/CycD3	YES	YES
S143	*in cellulo*		YES	YES
S146	IVK/*in cellulo*	ERK1+2	YES	YES
S151			YES	
T152			YES	YES
S165	IVK/*in cellulo*	ERK1+2, CDK4/CycD3	YES	YES
T170	IVK	ERK1+2	YES	YES
S178	IVK	PKCα		
T224				YES
S282	IVK	ERK1+2		YES
S285	IVK	ERK1+2, PKCα		
Y286	IVK	ERK1+2		
S301	IVK	ERK1+2		
T309	IVK/*in cellulo*	ERK1+2	YES	
S312	IVK/*in cellulo*	ERK1+2, CDK4/CycD3	YES	YES

IVK, *in vitro* kinase assay.

To investigate the impact of these mutations on integrin inhibition by SHARPIN, we used the previously reported fluorescence-activated cell sorting (FACS) assay (Bouaouina et al., 2011; Harburger et al., 2009). As expected, siRNA-mediated knockdown of SHARPIN in HeLa cells resulted in an increase in integrin activity (Fig. S1D), whereas overexpression of GFP-SHARPIN WT inhibited integrin activity in these SHARPIN-depleted cells (Fig. 2A). However, as both phospho-mutants also inhibited integrin activity, we conclude that these phosphorylation sites are not relevant for the ability of SHARPIN to inhibit integrins (Fig. 2A).

To analyze the effect of S131 and S146 phosphorylation sites on LUBAC activation, we used the NF-κB activity luciferase reporter assay in HeLa cells. As expected, loss of SHARPIN significantly reduced NF-κB activity (Fig. S1E), whereas overexpression of GFP-SHARPIN WT increased NF-κB activity (Fig. 2B). Consistent with a previous report (De Franceschi et al., 2015), the structural mutant L276A was unable to promote NF-κB activity (Fig. 2B). Notably, the S131A and S146A mutants were indistinguishable from SHARPIN WT in their capacity to promote NF-κB activity (Fig. 2B), demonstrating that, like their neutral effect on integrin activity, these phosphorylation sites are not involved in regulation of LUBAC activation.

SHARPIN has been identified to be an interactor of the ARP2/3 complex, and this interaction plays a role in ARP2/3-dependent lamellipodium formation, leading to possible regulation of cell migration (Khan et al., 2017). To investigate the effect of the mutations on the SHARPIN-ARP2/3 complex interaction, we analyzed fluorescence resonance energy transfer (FRET) efficiency between GFP-SHARPIN and ARP3-RFP in HeLa cells as described earlier (Fig. 2C) (Khan et al., 2017). As expected, no FRET signal was observed in cells with overexpression of GFP-SHARPIN WT alone, whereas a clear FRET signal was observed in cells with GFP-SHARPIN WT and ARP3-RFP co-expression (Fig. 2D). Interestingly, FRET activity in cells expressing GFP-SHARPIN S131A or S146A mutants was significantly lower than in the GFP-SHARPIN WT-expressing cells, and the activity with S146A was indistinguishable from that of the structural mutant V240A/L242A used as a negative control (De Franceschi et al., 2015). Out of these two mutations, S146A had clearly stronger effect on ARP3 interaction, and it was thus selected for further functional validation.

The results above indicate that S146 phosphorylation is critical for efficient SHARPIN-ARP2/3 interaction, but it is unclear whether this site is dynamically regulated by cellular signaling. To study this, we either inhibited the kinase predicted to phosphorylate S146 ERK1/2 by ravoxertinib, or used FTY720, which is a pharmacological activator of the major ERK1/2 serine/threonine phosphatase protein phosphatase 2A (PP2A) (Vainonen et al., 2021). As shown previously, co-expression of GFP-SHARPIN WT and ARP3-RFP resulted in a clear FRET signal, whereas a significant loss of FRET signal was observed between GFP-SHARPIN S146A and ARP3-RFP in untreated cells. Importantly, treatment with ravoxertinib completely abrogated the FRET signal. Furthermore, reactivation of PP2A by FTY720 caused a significant decrease in the FRET signal (Fig. 2E). Importantly, FTY720 did not further decrease interaction between GFP-SHARPIN S146A and ARP3-RFP, clearly suggesting that the impact of PP2A reactivation on GFP-SHARPIN WT interaction was mediated by dephosphorylation of S146 (Fig. 2E).

These results indicate that S146 phosphorylation of SHARPIN is under continuous regulation by the kinase-phosphatase balance between ERK1/2 and PP2A. The results also provide further validation of our MS and IVK results (Fig. 1, Table 1).

Constitutive SHARPIN S146 phosphorylation contributes to lamellipodium formation

ARP2/3-dependent lamellipodia formation promotes cell migration and invasion (Molinie and Gautreau, 2018; Mondal et al., 2021; Suraneni et al., 2012). We have previously shown that ARP2/3 interaction with SHARPIN promotes lamellipodia formation, but does not affect actin polymerization (Khan et al., 2017). Consistent with that study, siRNA-mediated knockdown of SHARPIN in NCI-H460 lung cancer cells significantly decreased lamellipodium formation and resulted in cells with rounded appearance (Fig. 3A). In a rescue experiment in which *SHARPIN*-silenced cells were transfected with either GFP only, GFP-SHARPIN WT, S146A or V240A/L242A double mutant as a negative control (Khan et al., 2017), only GFP-SHARPIN WT was able to rescue lamellipodium formation (Fig. 3B). These data are consistent with the FRET data (Fig. 2D), together indicating that phosphorylation of S146 is required for SHARPIN-mediated ARP2/3 activation.

Journal of Cell Science (2022) 135, jcs260627. doi:10.1242/jcs.260627

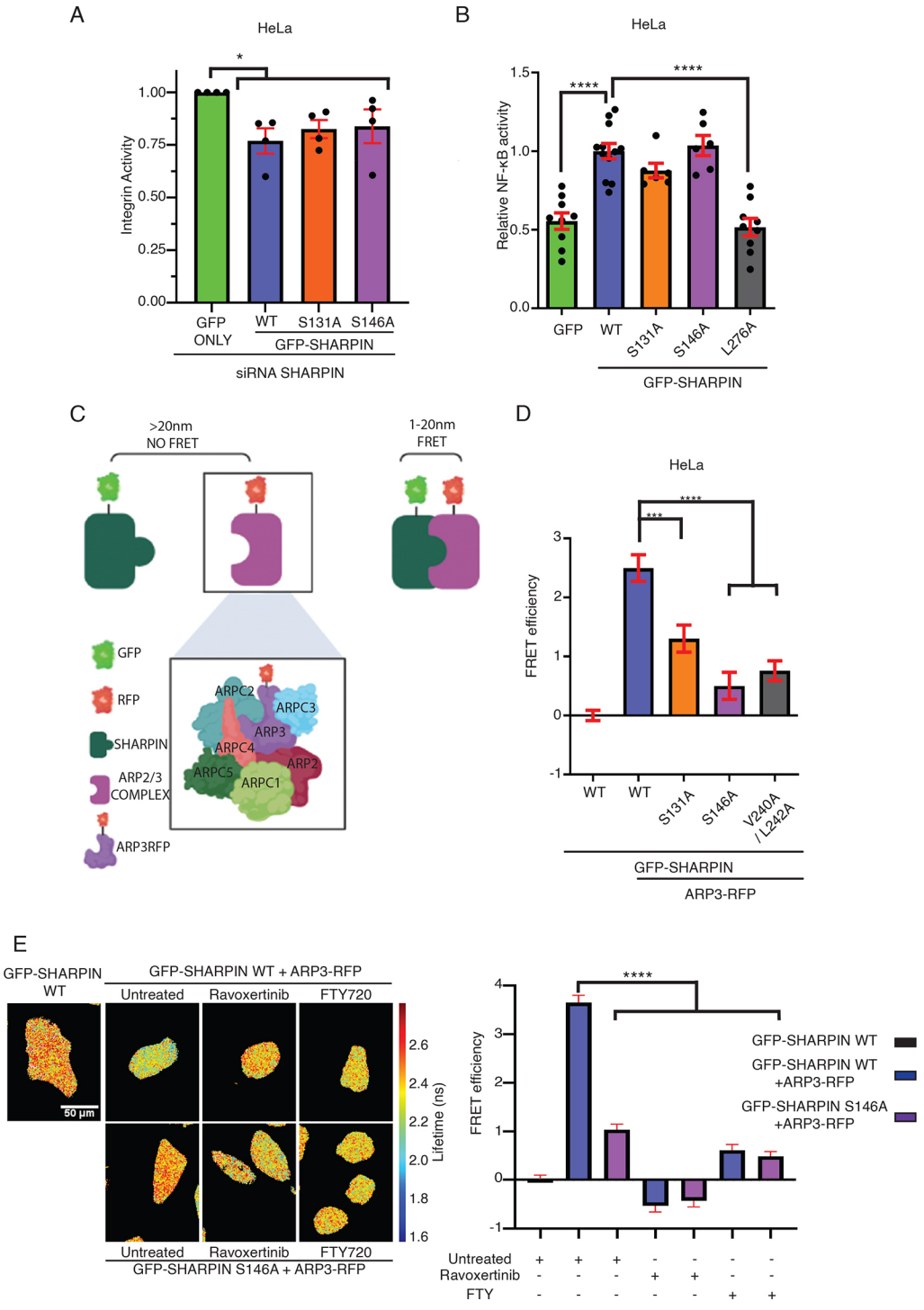

Fig. 2. SHARPIN S131 and S146 phosphorylation promotes interaction between SHARPIN and ARP2/3 complex. (A) Quantification of integrin activity in endogenous *SHARPIN*-silenced HeLa cells overexpressing the indicated SHARPIN variants in a fluorescence-activated cell sorting (FACS) assay (n=4 biological repeats). (B) TNF-induced NF-κB promoter activity in HeLa cells overexpressing indicated the SHARPIN variants. NF-κB promoter activity was measured using luciferase reporter assay. GFP-SHARPIN L276A was used as a negative control (n=6–12 measurements from three biological repeats). (C) Illustration of fluorescence resonance energy transfer (FRET) between GFP-SHARPIN and ARP3-RFP. (D) Quantification of FRET efficiency in HeLa cells overexpressing the indicated proteins subjected to FRET analysis by fluorescence lifetime imaging microscopy (FLIM) (n=≥22 cells). (E) MDA-MB-231 cells stably expressing either GFP-SHARPIN wild-type (WT) or GFP-SHARPIN S146A overexpressing ARP3-RFP were treated with the indicated drugs. Shown are fluorescence lifetimes of representative cells using a pseudo-color scale [red-yellow, normal lifetime; yellow-blue, FRET (reduced lifetime)]. Scale bar: 50 µm. Graphs show quantification of FRET efficiency of three biological repeats. Mann–Whitney test, mean±s.e.m., *P≤0.05, ***P≤0.001, ****P≤0.0001.

As S146 was found phosphorylated in the unperturbed cancer cells (Table 1), we assumed that overexpression of phosphomimic glutamate mutant of S146 (S146E) would not impact ARP2/3 interaction or lamellipodium formation by SHARPIN. Use of the S146E mutant would also be an important control that the impaired lamellipodia formation by S146A mutant was truly caused by lack of phosphorylation and not by structural impact of any random mutation. Importantly, although GFP-SHARPIN S146E showed slightly reduced binding to ARP3-RFP (Fig. 3C), its overexpression resulted in comparable rescue of lamellipodia formation compared to GFP-SHARPIN WT-expressing cells (Fig. 3D). Thereby, we conclude that the lack of lamellipodia rescue with the S146A mutant was due to impairment of phosphorylation at S146.

Both SHARPIN and ARP2/3 are reported to localize in lamellipodia (Khan et al., 2017) We analyzed intensities of GFP only, GFP-SHARPIN WT and the GFP-SHARPIN mutants, along with cortactin, to assess whether GFP-SHARPIN mutants differentially localize to the lamellipodia. Although overexpression of GFP-SHARPIN S146E or A146A phospho-mutants had differential effects on lamellipodia formation in NCI-H460 cells (Fig. 3B,D), this was not reflected in their enrichment at the lamellipodia, and actually no SHARPIN localization in those structures was observed even with the WT SHARPIN protein

Journal of Cell Science (2022) 135, jcs260627. doi:10.1242/jcs.260627

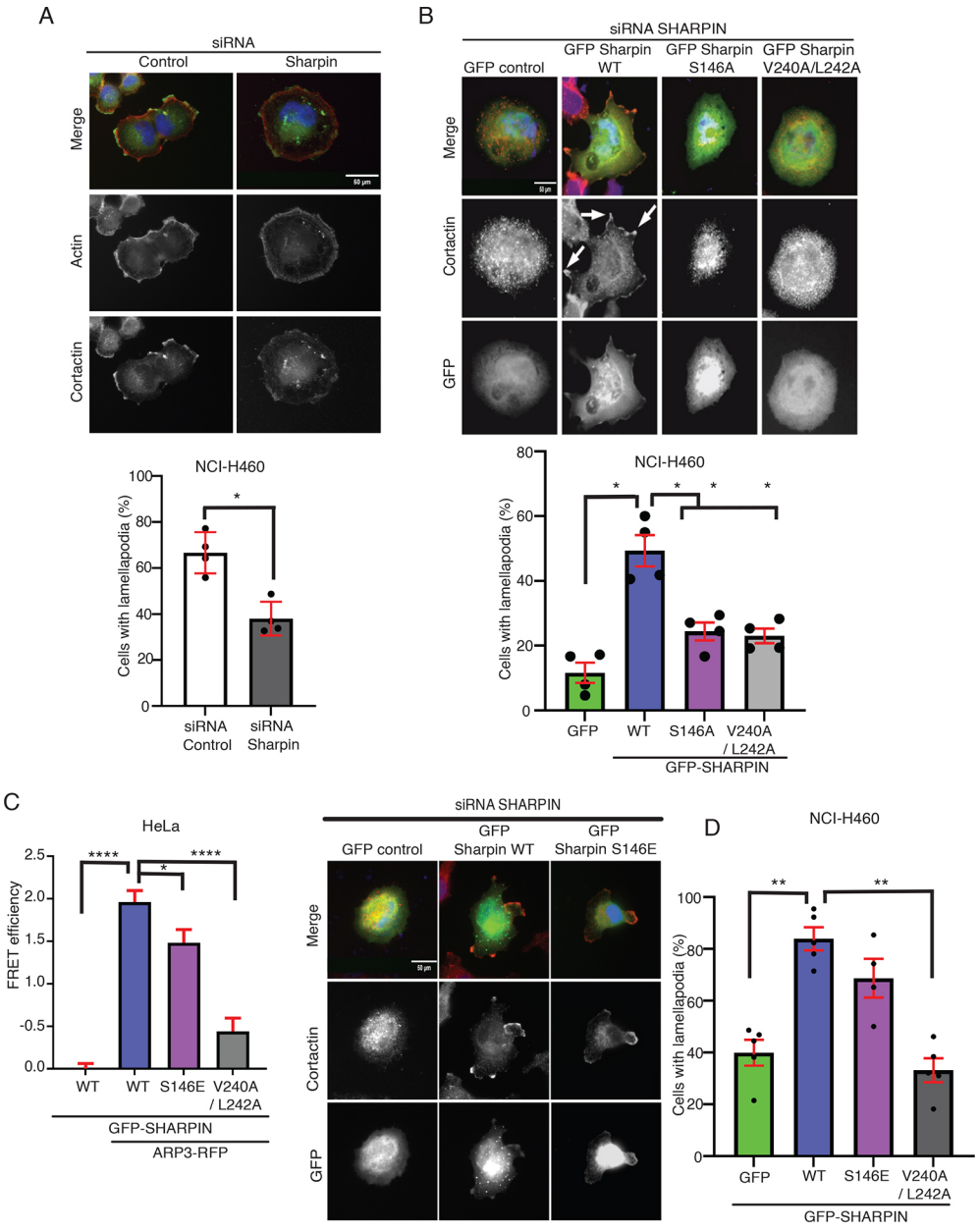

Fig. 3. Phosphorylation of SHARPIN at S146 promotes lamellipodia formation. (A) Impact of *SHARPIN* silencing on NCI- H460 cells' ability to form lamellipodia. Graph shows averages of quantification of cells with lamellipodia (n=4 biological repeats). (B) Lamellipodia formation in endogenous *SHARPIN*-silenced NCI-H460 cells overexpressing the indicated SHARPIN variants. GFP-SHARPIN V240A/L242A is used as a negative control. Graph shows averages of quantification of cells with lamellipodia (n=4 biological repeats). (C) Quantification of FRET efficiency in HeLa cells overexpressing the indicated proteins subjected to FRET analysis by FLIM (n=≥65 cells). (D) Lamellipodia formation in endogenous *SHARPIN*-silenced NCI-H460 cells overexpressing the indicated SHARPIN variants. GFP-SHARPIN V240A/L242A is used as a negative control. Graph shows averages of quantification of cells with lamellipodia (n=5 biological repeats). Mann–Whitney test, mean±s.e.m., *P≤0.05, **P≤0.01, ****P≤0.0001. Scale bars: 50 µm.

(Fig. S1F). These results demonstrate that the impact of GFP-SHARPIN mutations on lamellipodia formation does not involve differential recruitment to the lamellipodia, and suggest that it is rather mediated by ARP2/3 activation at other cellular compartments.

SHARPIN promotes three-dimensional (3D) cancer cell invasion

The ARP2/3 complex is a critical mediator of the entire metastatic cascade, from migration to invasion and *in vivo* metastatic spread (Molinie and Gautreau, 2018; Mondal et al., 2021). Based on the results above, we hypothesized that, owing to its impact on ARP2/3 complex interaction, S146 phosphorylation on SHARPIN promotes cancer cell invasiveness. This was particularly interesting as S146 phosphorylation selectively influenced lamellipodia formation without affecting the other studied signaling functions of SHARPIN (Fig. 2). To unambiguously study the function of SHARPIN in 3D invasion of cancer cells, we utilized CRISPR/Cas9-generated SHARPIN knockout (KO) NCI-H460 lung cancer cells generated previously (Khan et al., 2017), and created additional SHARPIN KO MDA-MB-231 triple-negative breast cancer cells and HeLa cervical cancer cells. Selection of these cell lines was due to high SHARPIN amplification frequency in these cancer types (Fig. S1A). After single-cell cloning of SHARPIN-targeted CRISPR/Cas9 clones, WB analysis was used to demonstrate complete loss of endogenous SHARPIN in the MDA-MB-231 and HeLa SHARPIN KO cells (Fig. S2A). Tracking the proliferation of MDA-MB-231 cell lines by IncuCyte live-cell imaging for 4 days revealed no significant differences (Fig. S2B). Therefore, the potential effects of knockout of SHARPIN in 3D invasion were not confounded by significant effects on cell proliferation.

The functional contribution of SHARPIN to 3D invasion was assessed using an inverted transwell invasion assay (Jacquemet et al., 2016). Remarkably, SHARPIN deletion was found essential for 3D invasion in all three cell lines (Fig. 4A–C). To rule out that

Journal of Cell Science (2022) 135, jcs260627. doi:10.1242/jcs.260627

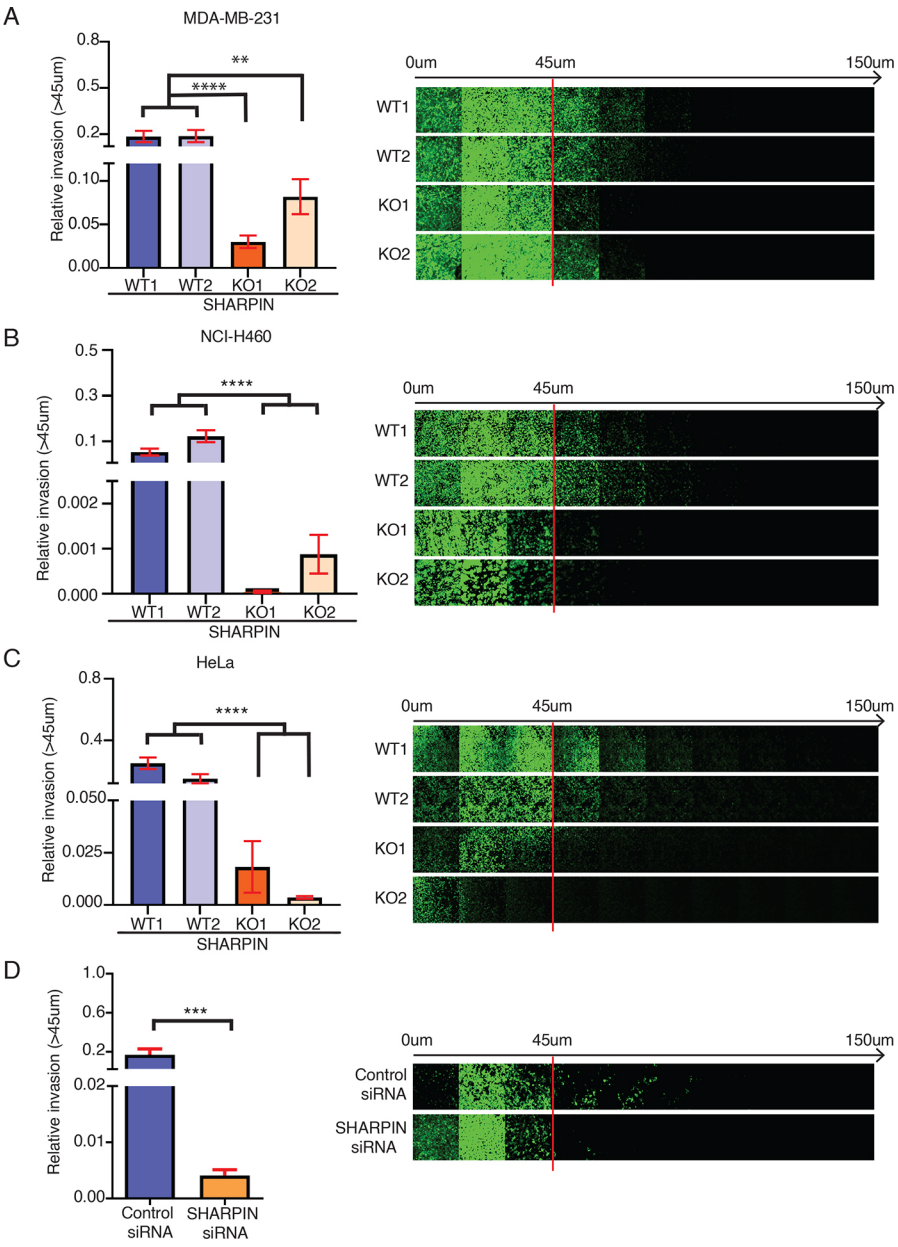

Fig. 4. SHARPIN is essential for cancer cell invasion. (A–C) Impact of endogenous SHARPIN knockout on an inverted 3D invasion assay in MDA-MB-231, NCI-H460 and HeLa cells generated by CRISPR/Cas9 gene editing (n=3 biological repeats). (D) Relative invasion in endogenous *SHARPIN*-silenced MDA-MB-231 cells (n=3 biological repeats). Mann–Whitney test, mean±s.e.m., $^{**}P\leq0.01$, $^{***}P\leq0.001$, $^{****}P\leq0.0001$.

this was not due to unspecific effect by the CRISPR/Cas9-mediated gene editing process, we repeated the assay with MDA-MB-231 cells from which SHARPIN was transiently knocked down by siRNA. Also in this setting, SHARPIN inhibition resulted in significant loss of invasion (Fig. 4D).

These results demonstrate an essential role for SHARPIN in 3D invasion of cancer cells in three different human cancer types with high amplification frequency of SHARPIN (Fig. S1A).

A single phosphorylation site, S146, on SHARPIN determines cancer cell invasiveness

The results above demonstrate that SHARPIN S146 phosphorylation promotes lamellipodia formation (Fig. 3), which is a known requirement for cancer cell invasion, and that SHARPIN is required for 3D invasion across cancer cell lines (Fig. 4). To investigate whether S146 phosphorylation of SHARPIN can alone define the ability of cancer cells to invade, the MDA-MB-231 SHARPIN KO clones were used to generate a cell line stably expressing either GFP only, GFP-SHARPIN WT or GFP-SHARPIN S146A mutant. Whereas negligible invasion was again seen with the KO cells in an inverted transwell invasion assay, complete rescue was seen in cells expressing GFP-SHARPIN WT. However, no rescue was observed in the cells expressing GFP-SHARPIN S146A mutant at the same level as GFP-SHARPIN WT (Fig. 5A; Fig. S2C). To rule out that these were clonal effects, and to expand the relevance of these findings to yet another cell model, the experiment was repeated in prostate cancer PC3 SHARPIN KO cells (Fig. 5B; Fig. S2D). Consistent with the results in MDA-MB-231 cells, significant rescue was observed in cells with overexpression of GFP-SHARPIN WT, whereas GFP-SHARPIN S146A mutant-expressing cells were indistinguishable from control GFP-expressing cells (Fig. 5C; Fig. S2D).

Finally, to investigate whether these results translate into invasion phenotype in animal model, we used the zebrafish model for cancer cell invasion (Teng et al., 2013). Zebrafish embryo hearts were injected with MDA-MB-231 cells stably expressing either GFP-SHARPIN WT or the GFP-SHARPIN S146A mutant. The embryos were then fixed and imaged on day 4 following the injection. Image

Journal of Cell Science (2022) 135, jcs260627. doi:10.1242/jcs.260627

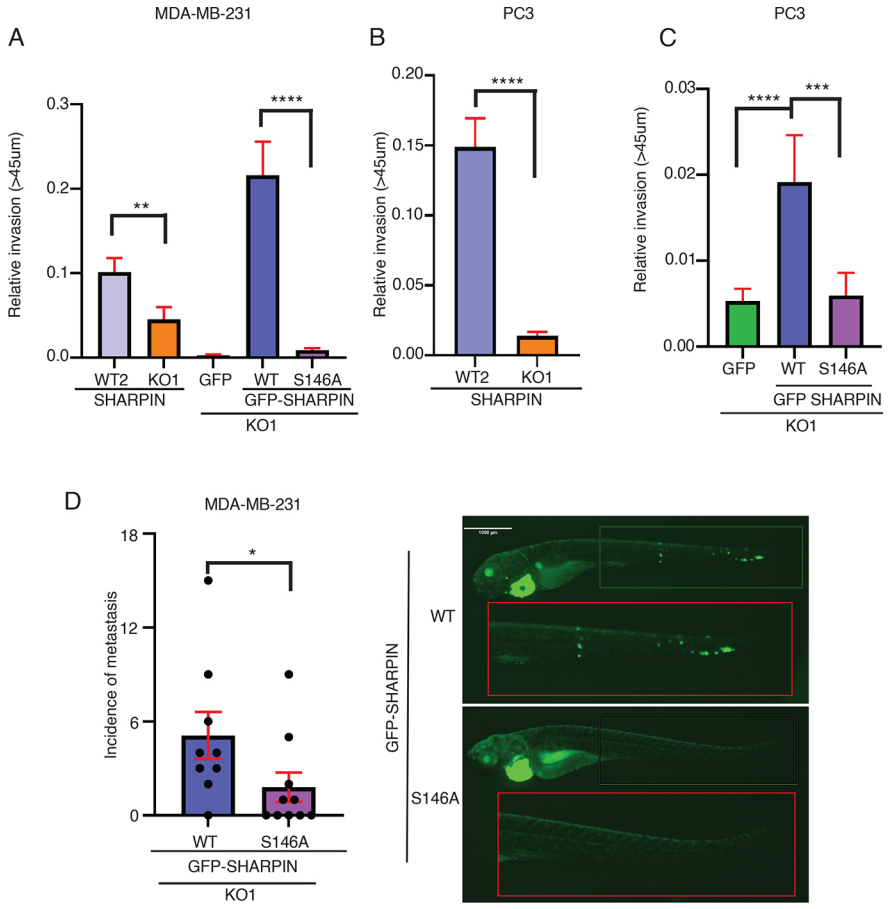

Fig. 5. SHARPIN S146 determines cancer cell invasion and metastasis. (A) 3D invasion of MDA-MB-231 SHARPIN knockout cells stably expressing GFP only, GFP-SHARPIN WT or GFP-SHARPIN S146A (n=3 biological repeats). (B) 3D invasion of prostate cancer PC3 cells with knockout of endogenous SHARPIN (n=3 biological repeats). (C) 3D invasion of PC3 SHARPIN knockout cells overexpressing GFP only, GFP-SHARPIN WT or GFP-SHARPIN S146A (n=3 biological repeats). (D) *In vivo* zebrafish metastasis of MDA-MB 231 cells stably expressing GFP-SHARPIN WT or GFP-SHARPIN S146A mutant at day 4 following heart injection. Scale bar: 1000 µm. Graph shows quantification of incidence of metastasis to zebrafish tail (n=10 zebrafish per group). Mann–Whitney test, mean±s.e.m., *P≤0.05, **P≤0.01, ***P≤0.001, ****P≤0.0001.

analysis revealed a significant decrease in distant tail metastases in embryos injected with GFP-SHARPIN S146A mutant cells compared to those injected with GFP-SHARPIN WT (Fig. 5D).

Collectively, these results demonstrate that SHARPIN S146 phosphorylation constitutes a functional determinant of 3D cancer cell invasion both *in vitro* and *in vivo*.

DISCUSSION

Metastasis is the primary cause of cancer-related deaths in most human solid malignancies. Thereby, identification of novel targets for anti-metastatic therapies could lead to profound decrease in cancer mortality and increased quality of life of cancer patients(Ganesh and Massagué, 2021). In this study, we demonstrate that SHARPIN is essential for 3D invasion of cancer cells in four different human cancer types, and that SHARPIN S146 phosphorylation functions as a critical invasion-promoting phosphorylation switch.

SHARPIN gene amplification and SHARPIN protein overexpression have been observed in several human cancer types (Fig. S1A) (Bii et al., 2015; De Melo and Tang, 2015; He et al., 2010; Jung et al., 2010). SHARPIN is a multifunctional protein regulating a number of cellular pathways and functions (Gerlach et al., 2011; He et al., 2010; Ikeda et al., 2011; Landgraf et al., 2010; Lim et al., 2001; Nastase et al., 2016; Park et al., 2016; Pouwels et al., 2013; Rantala et al., 2011; Tokunaga et al., 2011), and at least some of these roles of SHARPIN are mutually exclusive (De Franceschi et al., 2015). However, it has remained a mystery how the choice between different SHARPIN functions is controlled. Here, we addressed this question by comprehensive analysis of SHARPIN phosphorylation. By IVK, we demonstrated that SHARPIN is phosphorylated by major oncogenic kinases such as PKCα, CDK4/CycD3, ERK1 and ERK2. Through a combination of *in cellulo* phospho-proteomics analysis and database searches, we validated the amino acids that are constitutively phosphorylated in cancer cells (Table 1). These data provides a rich resource for future studies related to the role of different kinases and phosphatases in SHARPIN biology. For example, PKCα was recently shown to control cell motility and protrusion dynamics (Asokan et al., 2014), and it would be interesting in the future to study whether PKC-mediated SHARPIN phosphorylation (Fig. 1A, Table 1) contributes to these phenotypes. However, although previous study demonstrated the functional role of S165 phosphorylation in SHARPIN-mediated LUBAC regulation (Thys et al., 2021), the role of other SHARPIN phosphorylation sites has yet to be studied. Here, we focused on functional analysis of S131 and S146 phosphorylation, as these sites were observed to be phosphorylated both in MS and the IVK (Fig. 1C, Table 1).

Prior to this study, SHARPIN was known to promote lamellipodium formation through interaction with the ARP2/3 complex, and it was further demonstrated that this function was independent of its LUBAC- and integrin-related roles (Khan et al., 2017). Here, we demonstrate roles for S146 and S131 phosphorylation in SHARPIN-ARP2/3 interaction, and that mutations of these sites had no effect on the ability of SHARPIN to inhibit integrins or on NF-κB activation. S146 phosphorylation of SHARPIN was further validated to promote lamellipodia formation, but, consistent with constitutive phosphorylation of S146 based on MS data, the phosphorylation-mimicking mutation (S146E) functioned as a WT. Furthermore, we demonstrate that phosphorylation of SHARPIN at S146 translates into the ability of cancer cells to invade and to metastasize *in vivo*.

Journal of Cell Science (2022) 135, jcs260627. doi:10.1242/jcs.260627

In summary, our data indicate a single phosphorylation event – phosphorylation of SHARPIN at S146 – that is essential for tumor cell invasion. Clinically, this mechanism may at least partly contribute to the poor clinical outcome in patients with high SHARPIN expression. Therefore, future studies should be directed to validate S146 phosphorylation in patient samples in correlation with patient metastasis status. Related to development of future anti-metastatic therapies, our data provide very convincing evidence that inhibition of SHARPIN expression effectively abrogates 3D invasion across cells from different cancer types displaying *SHARPIN* gene amplification. Further, future structural analysis of ARP2/3 bound to the SHARPIN unstructured region between the PH and UBL domains could reveal important clues for potential targetability of this cancer cell invasion, promoting protein-protein interaction.

MATERIALS AND METHODS

Antibodies

The following antibodies were used: rabbit anti-SHARPIN (14626-1-AP, Proteintech; 1:1000 in WB), mouse anti-cortactin (p80/85) [05-180, Merck Millipore; 1:300 in immunofluorescence (IF)], mouse anti-GAPDH (5G4MaB6C5, HyTest; 1:20,000 in WB), Alexa Fluor 488 Phalloidin (Invitrogen; 1:300 in IF)

Secondary antibodies used were as follows: Alexa Fluor 488- or Alexa Fluor 555-conjugated IgGs (Invitrogen; IF), horseradish peroxidase (HRP)-conjugated IgGs (GE Healthcare; WB), DyLight 680- or 800-conjugated anti-mouse and rabbit IgGs (Thermo Fisher Scientific; WB), mouse P5D2 (Developmental Studies Hybridoma Bank; 1:20 in FACS), mouse 12G10 (ab30394, Abcam; 1:100 in FACS)

Plasmids and siRNAs

Construction of siRNA1-insensitive GFP-SHARPIN and SHARPIN mutant plasmids has been previously described (De Franceschi et al., 2015). The GFP-SHARPIN phospho-mutants were created by introducing point mutations in these vectors using site-directed mutagenesis. Construction of ARP3-TagRFP has been previously described (Khan et al., 2017). siRNAs were as follows: *SHARPIN* [Hs_SHARPIN_1 HP siRNA (Qiagen)] and control siRNA [AllStars negative control siRNA (Qiagen)]. All plasmids are available upon request.

Cells and transfections

HeLa cells were grown in Dulbecco's modified Eagle medium (DMEM) with 10% fetal bovine serum (FBS), 1% L-glutamine, 1% MEM non-essential amino acids, 1% sodium pyruvate, 2% HEPES and 1% penicillin-streptomycin. HEK-293 cells were grown in DMEM with 1% penicillin-streptomycin, 10% FBS and 1% L-glutamine. NCI-H460 cells were grown in RPMI1640 with 10% FBS, 1% penicillin-streptomycin, 1% L-glutamine, 1% MEM non-essential amino acids, 1% sodium pyruvate and 1% glucose. MDA-MB-231 cells were grown in DMEM with 10% FBS, 1% L-glutamine and 1% penicillin-streptomycin. PC3 cells were grown in RPMI with 10% FBS, 1% penicillin-streptomycin and 1% L-glutamine. All cell lines were regularly tested for contaminations and were from American Type Culture Collection (ATCC). Plasmid transfections were performed using Lipofectamine 2000 (HeLa and HEK-293 cells), Lipofectamine 3000 (NCI-H460 cells) (Life Technologies) and jetPRIME (MDA-MB-231 and PC3 cells). siRNA transfections were performed using Hiperfect (Qiagen).

Recombinant proteins

Recombinant GST and GST-SHARPIN were produced in *Escherichia coli* Rosetta BL21DE3 and purified according to the manufacturer's instructions (BD Biosciences).

IVK and MS

Recombinant kinases were purchased from ProQinase GmbH. Twenty nanograms of kinase were mixed with 1 µg GST-SHARPIN and incubated in 20 mM Hepes (pH 7.4), 10 mM $CaCl_2$, 25 mM $MgCl_2$, 1 mM ATP and 5 µCi 32P-γ-ATP. Samples were then incubated on a heat block for 1 h at 30°C. Kinase reaction was terminated using 2× Laemmli (SDS) sample buffer. Samples were then boiled at 100°C for 10 min and run on a gel. Coomassie Blue-stained SDS-PAGE gel bands of GST-SHARPIN were then cut out for MS, and protein samples were digested by trypsin. Phosphopeptide enrichment was done by TiO_2 chromatography. Liquid chromatography-tandem MS (LC-MS/MS) analysis was done using Q Exactive (a quadrupole-orbitrap mass spectrometer). Data analysis was done using Mascot database search against SwissProt *E. coli* supplemented with GST-tagged SHARPIN and common contaminants.

For *in cellulo* analysis of SHARPIN phosphorylation, GFP pulldowns were performed using GFP-Trap beads (ChromoTek) according to the manufacturer's protocol. GFP-SHARPIN had been isolated by immunoprecipitation using beads and separated by SDS-PAGE. GFP-SHARPIN was in-gel digested by trypsin. Digested and desalted peptide samples were dissolved in 1% formic acid and analyzed by LC-electrospray ionization (ESI)-MS/MS using a Q Exactive mass spectrometer. The LC-ESI-MS/MS analyses were performed on a nanoflow HPLC system (Easy-nLC1000, Thermo Fisher Scientific) coupled to a Q Exactive mass spectrometer (Thermo Fisher Scientific, Bremen, Germany) equipped with a nano-electrospray ionization source. Peptides were first loaded on a trapping column and subsequently separated inline on a 15 cm C18 column (75 µm×15 cm, ReproSil-Pur 5 µm 200 Å C18-AQ, Dr. Maisch HPLC GmbH, Ammerbuch-Entringen, Germany). The mobile phase consisted of water with 0.1% formic acid (solvent A) and acetonitrile/water [80:20 (v/v)] with 0.1% formic acid (solvent B). A linear 10 min gradient from 8% to 43% B was used to elute peptides. MS data were acquired automatically using Thermo Xcalibur 3.0 software (Thermo Fisher Scientific). An information-dependent acquisition method consisted of an Orbitrap MS survey scan of mass range 300-2000 m/z followed by higher-energy C-trap dissociation (HCD) fragmentation for the ten most intense peptide ions.

The data files were searched for protein identification using Proteome Discoverer 1.4 software (Thermo Fisher Scientific) connected to an in-house server running Mascot 2.4.1 software (Matrix Science) against SwissProt_2016_01 database. PhosphoRS 3.1 tool was used for detecting localization of phosphorylation sites.

FACS

HeLa cells were seeded onto a six-well plate. The next day, cells were transfected with control or *SHARPIN* siRNA. The following day, these cells were transfected with GFP control, GFP-SHARPIN WT, GFP-SHARPIN S131A or GFP-SHARPIN S146A. The subsequent day, cells were harvested and fixed with 4% paraformaldehyde (PFA). Cells were stained for active β1-integrin (12G10) or total β1-integrin (P5D2). Samples were analyzed using FACSCalibur with CellQuest software (BD Biosciences) and non-commercial Flowing Software ver. 2.5 (Perttu Terho; Turku Centre for Biotechnology, Finland; www.flowingsoftware.com). The integrin activation index was calculated by dividing the background-corrected active cell-surface integrin levels by total cell-surface integrin levels.

NF-κB reporter assay

HeLa cells were seeded onto a six-well plate. The following day, these cells were transfected with Renilla Luciferase control vector (pRLTK), NF-κB reporter plasmid [pGL4.32(luc2P/NF-κB-RE/Hygro)] and WT or mutant GFP-SHARPIN expression plasmids. A GFP-only expression vector was used as a negative control. The next day, medium was replaced with medium with or without 50 ng/ml TNF, and, after 5 h, luciferase activity was measured using a Dual-Luciferase Reporter Assay System (Promega), according to the manufacturer's instructions. Luminescence detection was done using a Synergy H1 Multi-Mode Reader.

FRET measurements by FLIM

HeLa cells were transfected with donor alone [GFP-SHARPIN constructs (WT, or phospho-mutants) or with donor together with the acceptor (ARP3-TagRFP). Cells were fixed 24 h post-transfection and mounted with Mowiol 4-88 (Sigma-Aldrich). GFP fluorescence lifetime was measured using a fluorescence lifetime imaging attachment (Lambert Instruments) on a Zeiss AXIO Observer D1 inverted microscope. For sample excitation, a

sinusoidally modulated 3 W, 497 nm LED at 40 MHz under epi-illumination was used. Cells were imaged using the 63×/1.4 NA oil objective (excitation, BP470/40; beam splitter, FT495; emission, BP525/50). The phase and modulation were determined using the manufacturer's software from images acquired at 12-phase settings. Fluorescein at 0.01 mM, pH 9 was used as a lifetime reference standard. The FRET efficiency was calculated as previously described (Khan et al., 2017).

IF

NCI-H460 cells were seeded in a six-well plate. The next day, cells were transfected with control or *SHARPIN* siRNA. The following day, cells were trypsinized and re-seeded onto coverslips in a 24-well plate. The subsequent day, the cells were transfected with GFP control, GFP-SHARPIN WT, GFP-SHARPIN S146A or GFP-SHARPIN S146E and GFP-SHARPIN V240A/L242A. Cells were fixed with 4% PFA for 15 min at room temperature the following day. Permeabilization of cells was done with 0.1% Triton-X 100. Blocking was done with 10% goat serum. Cells were then stained with mouse anti-cortactin (p80/85) overnight at 4°C. Cells were imaged using a Zeiss AxioVert 200 M inverted wide-field microscope equipped with a Plan-NEOFLUAR 63×/1.25 NA oil objective (Zeiss) and Orca-ER camera (Hamamatsu Photonics). Image processing was performed using Fiji image analysis software (Schindelin et al., 2012).

SHARPIN knockout cell lines created with CRISPR

The SHARPIN knockout NCI-H460 cell line was previously generated (Khan et al., 2017). SHARPIN knockout cell lines (MDA-MB-231, HeLa, PC3) were created using CRISPR genome engineering as previously described (Khan et al., 2017).

WB

For assessing GFP-SHARPIN WT and mutants' expression levels, HeLa cells were seeded onto a six-well plate. The next day, the cells were transfected with GFP only, GFP-SHARPIN WT and mutant constructs. Forty-eight hours post-transfection, cells were harvested, lysed and run in SDS-PAGE. Proteins were transferred to nitrocellulose membranes and probed with anti-GFP and anti-GAPDH antibodies. For validation of SHARPIN CRISPR knockouts, respective cell lines were grown on six-well plates and harvested for western blots. Membranes were probed with anti-SHARPIN and anti-GAPDH antibodies.

Cell proliferation

MDA-MB-231 SHARPIN CRISPR WT and KO cells were seeded onto a 96-well plate (1000 cells per well). Cells were then imaged every 2 h using an IncuCyte Zoom™ System (Essen BioScience) with a 10× objective for 4 days.

Inverted invasion assay

Inverted invasion assays have been previously described (Jacquemet et al., 2016). Collagen 1 (concentration 5 µg/ml; PureCol EZ Gel, Advanced BioMatrix) supplemented with fibronectin (25 µg/ml) was incubated at 1 h at 37°C to polymerize it in the inserts (8 µm ThinCert, Greiner Bio-One). Inserts were then inverted, and cells were seeded on the opposite side of the filter and allowed to attach to the matrix for 4 h at 37°C. The inserts were then placed in serum-free medium. Medium supplemented with 10% FBS was placed on top of the matrix in the inserts, providing a serum gradient. Cells were fixed after 24–48 h of seeding; 4% PFA was used to fix cells for 2 h. Cell permeabilization was done using 0.5% Triton-X 100 at room temperature for 30 min. Cells were stained with Alexa Fluor 488 Phalloidin overnight at 4°C. Following staining, the plugs were washed three times with PBS and imaged on a confocal microscope (LAM510, LSM 780, LSM 880; Zeiss). *Z*-stacks of the samples were captured with a slice interval of 15 µm using a 20×/0.50 NA objective lens (air, Plan-Neofluar). A montage of the individual confocal images is presented, showing increasing penetrance from left to right. Invasion of cells was calculated using the area calculator plugin in ImageJ. The fluorescence intensity of cells invading more than 45 µm was used to calculate the percentage of cells in the plug that were able to invade.

Zebrafish embryo xenograft

Zebrafish were injected with MDA-MB-231 cells stably expressing either GFP-SHARPIN WT or GFP SHARPIN S146A mutant cells according to the previously described protocol (Paatero et al., 2018). Following transplantation, embryos were imaged the next day using a Zeiss SteREO Lumar.V12 microscope. After 4 days, the embryos were imaged again. Image analysis was done using Fiji image analysis software (Schindelin et al., 2012). Cell populations representing distant metastasis were counted manually.

Statistical analysis

All statistical analyses were performed using Prism version 9 for Windows (GraphPad Software). For all data, the Mann–Whitney test was used. $P \leq 0.05$ was considered significant.

Acknowledgements

The authors thank Taina Kalevo-Mattila for technical assistance and the entire Turku Bioscience personnel. We acknowledge the Cell Imaging and Cytometry core facility, Proteomics core facility and Zebrafish core facility at Turku Bioscience Center supported by Biocenter Finland.

Competing interests

The authors declare no competing or financial interests.

Author contributions

Conceptualization: U.B., J.P., J.W.; Methodology: U.B.; Software: U.B.; Validation: U.B.; Formal analysis: U.B.; Investigation: U.B., M.H.K.; Resources: J.P., J.W.; Data curation: U.B.; Writing - original draft: U.B., J.W.; Writing - review & editing: U.B., J.W.; Visualization: U.B.; Supervision: J.P., J.W.; Funding acquisition: J.P., J.W.

Funding

This project was funded by Academy of Finland (to J.P.), Syöpäsäätiö (to J.W.) and Sigrid Juséliuksen Säätiö (to J.W.). U.B. was supported by Suomen Kulttuurirahasto and K. Albin Johanssons Stiftelse. Open Access funding provided by Turun Yliopisto. Deposited in PMC for immediate release.

Peer review history

The peer review history is available online at https://journals.biologists.com/jcs/article-lookup/doi/10.1242/jcs.260627.

References

Asokan, S. B., Johnson, H. E., Rahman, A., King, S. J., Rotty, J. D., Lebedeva, I. P., Haugh, J. M. and Bear, J. E. (2014). Mesenchymal chemotaxis requires selective inactivation of myosin II at the leading edge via a noncanonical PLCγ/PKCα pathway. *Dev. Cell* **31**, 747-760. doi:10.1016/j.devcel.2014.10.024

Bii, V. M., Rae, D. T. and Trobridge, G. D. (2015). A novel gammaretroviral shuttle vector insertional mutagenesis screen identifies SHARPIN as a breast cancer metastasis gene and prognostic biomarker. *Oncotarget* **6**, 39507-39520. doi:10.18632/oncotarget.6232

Blanchoin, L., Amann, K. J., Higgs, H. N., Marchand, J. B., Kaiser, D. A. and Pollard, T. D. (2000). Direct observation of dendritic actin filament networks nucleated by Arp2/3 complex and WASP/Scar proteins. *Nature* **404**, 1007-1011. doi:10.1038/35010008

Bouaouina, M., Harburger, D. S. and Calderwood, D. A. (2011). Talin and signaling through integrins. In *Integrin and Cell Adhesion Molecules, Methods in Molecular Biology, vol. 757* (ed. Shimaoka, M.), pp. 325-347, doi:10.1007/978-1-61779-166-6_20. Totowa, NJ: Humana Press.

Chen, L., Liu, S. and Tao, Y. (2020). Regulating tumor suppressor genes: post-translational modifications. *Signal Transduct. Target. Ther.* **5**, 90. doi:10.1038/s41392-020-0196-9

De Franceschi, N., Peuhu, E., Parsons, M., Rissanen, S., Vattulainen, I., Salmi, M., Ivaska, J. and Pouwels, J. (2015). Mutually exclusive roles of SHARPIN in integrin inactivation and NF-κB signaling. *PLoS One* **10**, e0143423. doi:10.1371/journal.pone.0143423

De Melo, J. and Tang, D. (2015). Elevation of SIPL1 (SHARPIN) increases breast cancer risk. *PLoS One* **10**, e0127546. doi:10.1371/journal.pone.0127546

De Melo, J., Wu, V., He, L., Yan, J. and Tang, D. (2014). SIPL1 enhances the proliferation, attachment, and migration of CHO cells by inhibiting PTEN function. *Int. J. Mol. Med.* **34**, 835-841. doi:10.3892/ijmm.2014.1840

Fares, J., Fares, M. Y., Khachfe, H. H., Salhab, H. A. and Fares, Y. (2020). Molecular principles of metastasis: a hallmark of cancer revisited. *Signal Transduct. Target. Ther.* **5**, 28. doi:10.1038/s41392-020-0134-x

Ganesh, K. and Massagué, J. (2021). Targeting metastatic cancer. *Nat. Med.* **27**, 34-44. doi:10.1038/s41591-020-01195-4

Gao, J., Bao, Y., Ge, S., Sun, P., Sun, J., Liu, J., Chen, F., Han, L., Cao, Z., Qin, J. et al. (2019). Sharpin suppresses β1-integrin activation by complexing with the β1 tail and kindlin-1. *Cell Commun. Signal.* **17**, 101. doi:10.1186/s12964-018-0315-1

Gerlach, B., Cordier, S. M., Schmukle, A. C., Emmerich, C. H., Rieser, E., Haas, T. L., Webb, A. I., Rickard, J. A., Anderton, H., Wong, W. W.-L. et al. (2011). Linear ubiquitination prevents inflammation and regulates immune signalling. *Nature* **471**, 591-596. doi:10.1038/nature09816

Guan, X. (2015). Cancer metastases: challenges and opportunities. *Acta Pharm. Sin. B* **5**, 402-418. doi:10.1016/j.apsb.2015.07.005

Harburger, D. S., Bouaouina, M. and Calderwood, D. A. (2009). Kindlin-1 and-2 directly bind the C-terminal region of β integrin cytoplasmic tails and exert integrin-specific activation effects. *J. Biol. Chem.* **284**, 11485-11497. doi:10.1074/jbc.M809233200

He, L., Ingram, A., Rybak, A. P. and Tang, D. (2010). Shank-interacting protein–like 1 promotes tumorigenesis via PTEN inhibition in human tumor cells. *J. Clin. Invest.* **120**, 2094-2108. doi:10.1172/JCI40778

Ikeda, F., Deribe, Y. L., Skånland, S. S., Stieglitz, B., Grabbe, C., Franz-Wachtel, M., Van Wijk, S. J., Goswami, P., Nagy, V., Terzic, J. et al. (2011). SHARPIN forms a linear ubiquitin ligase complex regulating NF-κB activity and apoptosis. *Nature* **471**, 637-641. doi:10.1038/nature09814

Iwaya, K., Oikawa, K., Semba, S., Tsuchiya, B., Mukai, Y., Otsubo, T., Nagao, T., Izumi, M., Kuroda, M. and Domoto, H. (2007). Correlation between liver metastasis of the colocalization of actin–related protein 2 and 3 complex and WAVE2 in colorectal carcinoma. *Cancer Sci.* **98**, 992-999. doi:10.1111/j.1349-7006.2007.00488.x

Jacquemet, G., Baghirov, H., Georgiadou, M., Sihto, H., Peuhu, E., Cettour-Janet, P., He, T., Perälä, M., Kronqvist, P., Joensuu, H. et al. (2016). L-type calcium channels regulate filopodia stability and cancer cell invasion downstream of integrin signalling. *Nat. Commun.* **7**, 13297. doi:10.1038/ncomms13297

Jung, J., Kim, J. M., Park, B., Cheon, Y., Lee, B., Choo, S. H., Koh, S. S. and Lee, S. (2010). Newly identified tumor-associated role of human Sharpin. *Mol. Cell. Biochem.* **340**, 161-167. doi:10.1007/s11010-010-0413-x

Kashani-Sabet, M., Rangel, J., Torabian, S., Nosrati, M., Simko, J., Jablons, D. M., Moore, D. H., Haqq, C., Miller, J. R. and Sagebiel, R. W. (2009). A multi-marker assay to distinguish malignant melanomas from benign nevi. *Proc. Natl. Acad. Sci. USA* **106**, 6268-6272. doi:10.1073/pnas.0901185106

Khan, M. H., Salomaa, S. I., Jacquemet, G., Butt, U., Miihkinen, M., Deguchi, T., Kremneva, E., Lappalainen, P., Humphries, M. J. and Pouwels, J. (2017). The Sharpin interactome reveals a role for Sharpin in lamellipodium formation via the Arp2/3 complex. *J. Cell Sci.* **130**, 3094-3107. doi:10.1242/jcs.200329

Landgraf, K., Bollig, F., Trowe, M.-O., Besenbeck, B., Ebert, C., Kruspe, D., Kispert, A., Hänel, F. and Englert, C. (2010). Sipl1 and Rbck1 are novel Eya1-binding proteins with a role in craniofacial development. *Mol. Cell. Biol.* **30**, 5764-5775. doi:10.1128/MCB.01645-09

Li, J., Lai, Y., Cao, Y., Du, T., Zeng, L., Wang, G., Chen, X., Chen, J., Yu, Y., Zhang, S. et al. (2015). SHARPIN overexpression induces tumorigenesis in human prostate cancer LNCaP, DU145 and PC-3 cells via NF-κB/ERK/Akt signaling pathway. *Med. Oncol.* **32**, 444. doi:10.1007/s12032-014-0444-3

Lim, S., Sala, C., Yoon, J., Park, S., Kuroda, S. i., Sheng, M. and Kim, E. (2001). Sharpin, a novel postsynaptic density protein that directly interacts with the shank family of proteins. *Mol. Cell. Neurosci.* **17**, 385-397. doi:10.1006/mcne.2000.0940

Liu, Z., Yang, X., Chen, C., Liu, B., Ren, B., Wang, L., Zhao, K., Yu, S. and Ming, H. (2013). Expression of the Arp2/3 complex in human gliomas and its role in the migration and invasion of glioma cells. *Oncol. Rep.* **30**, 2127-2136. doi:10.3892/or.2013.2669

Liu, J., Wang, Y., Gong, Y., Fu, T., Hu, S., Zhou, Z. and Pan, L. (2017). Structural insights into SHARPIN-mediated activation of HOIP for the linear ubiquitin chain assembly. *Cell Rep.* **21**, 27-36. doi:10.1016/j.celrep.2017.09.031

Molinie, N. and Gautreau, A. (2018). The Arp2/3 regulatory system and its deregulation in cancer. *Physiol. Rev.* **98**, 215-238. doi:10.1152/physrev.00006.2017

Mondal, C., Di Martino, J. S. and Bravo-Cordero, J. J. (2021). Actin dynamics during tumor cell dissemination. *Int. Rev. Cell Mol. Biol.* **360**, 65-98. doi:10.1016/bs.ircmb.2020.09.004

Nastase, M.-V., Zeng-Brouwers, J., Frey, H., Hsieh, L. T.-H., Poluzzi, C., Beckmann, J., Schroeder, N., Pfeilschifter, J., Lopez-Mosqueda, J., Mersmann, J. et al. (2016). An essential role for SHARPIN in the regulation of caspase 1 activity in sepsis. *Am. J. Pathol.* **186**, 1206-1220. doi:10.1016/j.ajpath.2015.12.026

Nishi, H., Hashimoto, K. and Panchenko, A. R. (2011). Phosphorylation in protein-protein binding: effect on stability and function. *Structure* **19**, 1807-1815. doi:10.1016/j.str.2011.09.021

Otsubo, T., Iwaya, K., Mukai, Y., Mizokami, Y., Serizawa, H., Matsuoka, T. and Mukai, K. (2004). Involvement of Arp2/3 complex in the process of colorectal carcinogenesis. *Mod. Pathol.* **17**, 461-467. doi:10.1038/modpathol.3800062

Paatero, I., Alve, S., Gramolelli, S., Ivaska, J. and Ojala, P. M. (2018). Zebrafish embryo xenograft and metastasis assay. *Bio-protocol* **8**, e3027. doi:10.21769/BioProtoc.3027

Park, Y., Jin, H.-S., Lopez, J., Lee, J., Liao, L., Elly, C. and Liu, Y.-C. (2016). SHARPIN controls regulatory T cells by negatively modulating the T cell antigen receptor complex. *Nat. Immunol.* **17**, 286-296. doi:10.1038/ni.3352

Pouwels, J., De Franceschi, N., Rantakari, P., Auvinen, K., Karikoski, M., Mattila, E., Potter, C., Sundberg, J. P., Hogg, N., Gahmberg, C. G. et al. (2013). SHARPIN regulates uropod detachment in migrating lymphocytes. *Cell Rep.* **5**, 619-628. doi:10.1016/j.celrep.2013.10.011

Rana, P. S., Alkrekshi, A., Wang, W., Markovic, V. and Sossey-Alaoui, K. (2021). The Role of WAVE2 Signaling in Cancer. *Biomedicines* **9**, 1217. doi:10.3390/biomedicines9091217

Rantala, J. K., Pouwels, J., Pellinen, T., Veltel, S., Laasola, P., Mattila, E., Potter, C. S., Duffy, T., Sundberg, J. P., Kallioniemi, O. et al. (2011). SHARPIN is an endogenous inhibitor of β1-integrin activation. *Nat. Cell Biol.* **13**, 1315-1324. doi:10.1038/ncb2340

Schindelin, J., Arganda-Carreras, I., Frise, E., Kaynig, V., Longair, M., Pietzsch, T., Preibisch, S., Rueden, C., Saalfeld, S., Schmid, B. et al. (2012). Fiji: an open-source platform for biological-image analysis. *Nat. Methods* **9**, 676-682. doi:10.1038/nmeth.2019

Semba, S., Iwaya, K., Matsubayashi, J., Serizawa, H., Kataba, H., Hirano, T., Kato, H., Matsuoka, T. and Mukai, K. (2006). Coexpression of actin-related protein 2 and Wiskott-Aldrich syndrome family verproline-homologous protein 2 in adenocarcinoma of the lung. *Clin. Cancer Res.* **12**, 2449-2454. doi:10.1158/1078-0432.CCR-05-2566

Steeg, P. S. (2016). Targeting metastasis. *Nat. Rev. Cancer* **16**, 201-218. doi:10.1038/nrc.2016.25

Suraneni, P., Rubinstein, B., Unruh, J. R., Durnin, M., Hanein, D. and Li, R. (2012). The Arp2/3 complex is required for lamellipodia extension and directional fibroblast cell migration. *J. Cell Biol.* **197**, 239-251. doi:10.1083/jcb.201112113

Teng, Y., Xie, X., Walker, S., White, D. T., Mumm, J. S. and Cowell, J. K. (2013). Evaluating human cancer cell metastasis in zebrafish. *BMC Cancer* **13**, 453. doi:10.1186/1471-2407-13-453

Thys, A., Trillet, K., Rosińska, S., Gayraud, A., Douanne, T., Danger, Y., Renaud, C. C., Antigny, L., Lavigne, R., Pineau, C. et al. (2021). Serine 165 phosphorylation of SHARPIN regulates the activation of NF-κB. *Iscience* **24**, 101939. doi:10.1016/j.isci.2020.101939

Tokunaga, F., Nakagawa, T., Nakahara, M., Saeki, Y., Taniguchi, M., Sakata, S.-i., Tanaka, K., Nakano, H. and Iwai, K. (2011). SHARPIN is a component of the NF-κB-activating linear ubiquitin chain assembly complex. *Nature* **471**, 633-636. doi:10.1038/nature09815

Vainonen, J. P., Momeny, M. and Westermarck, J. (2021). Druggable cancer phosphatases. *Sci. Transl. Med.* **13**, eabe2967. doi:10.1126/scitranslmed.abe2967

Zhang, Y., Guan, X.-Y., Dong, B., Zhao, M., Wu, J.-H., Tian, X.-Y. and Hao, C.-Y. (2012). Expression of MMP-9 and WAVE3 in colorectal cancer and its relationship to clinicopathological features. *J. Cancer Res. Clin. Oncol.* **138**, 2035-2044. doi:10.1007/s00432-012-1274-3

Zhang, Y., Huang, H., Zhou, H., Du, T., Zeng, L., Cao, Y., Chen, J., Lai, Y., Li, J., Wang, G. et al. (2014). Activation of nuclear factor κB pathway and downstream targets survivin and livin by SHARPIN contributes to the progression and metastasis of prostate cancer. *Cancer* **120**, 3208-3218. doi:10.1002/cncr.28796

Zhou, S., Liang, Y., Zhang, X., Liao, L., Yang, Y., Ouyang, W. and Xu, H. (2020). SHARPIN promotes melanoma progression via Rap1 signaling pathway. *J. Investig. Dermatol.* **140**, 395-403.e6. doi:10.1016/j.jid.2019.07.696